

Ligand recognition and allosteric modulation of the human MRGPRX1 receptor

In the format provided by the authors and unedited

Ligand recognition and allosteric modulation of the human

MRGPRX1 receptor

Yongfeng Liu^{1,2,7}, Can Cao^{1,7}, Xi-Ping Huang^{1,2}, Ryan H. Gumpfer¹, Moira M. Rachman³, Sheng-Luen Shih^{1,2}, Brian E. Krumm¹, Shicheng Zhang¹, Brian K. Shoichet³, Jonathan F. Fay^{4,5*} and Bryan L. Roth^{1,2,6*}

¹ Department of Pharmacology, University of North Carolina School of Medicine, Chapel Hill, NC 27599, USA

² National Institute of Mental Health Psychoactive Drug Screening Program, University of North Carolina School of Medicine, Chapel Hill, NC 27599, USA

³ Department of Pharmaceutical Sciences, University of California San Francisco, School of Medicine, San Francisco, CA 94158, USA

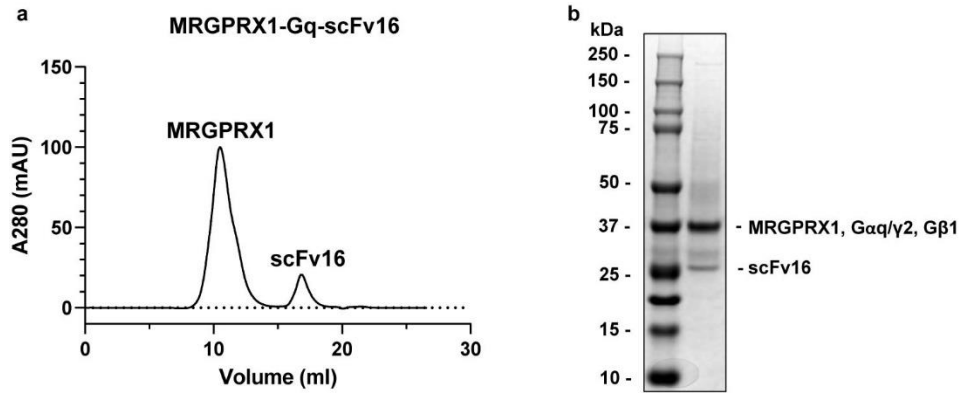
⁴ Department of Biochemistry and Biophysics, University of North Carolina School of Medicine, Chapel Hill, NC 27599, USA

⁵ Present address: Department of Biochemistry and Molecular Biology, University of Maryland School of Medicine, Baltimore, MD 21201, USA

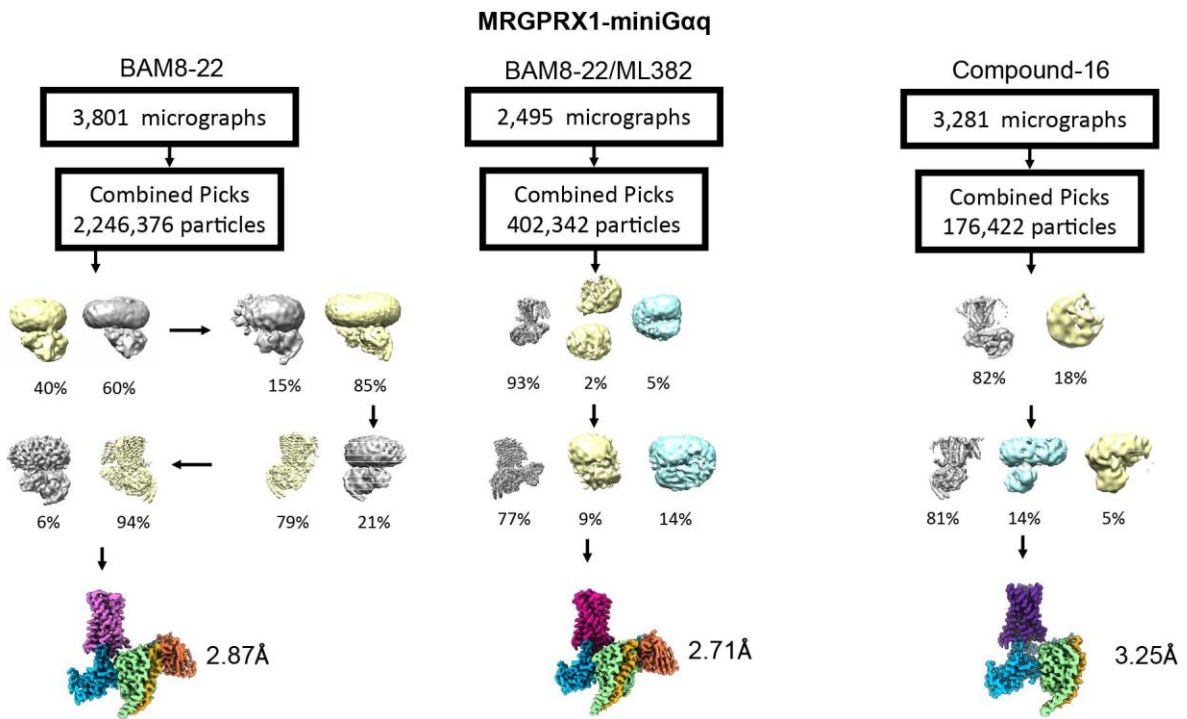
⁶ Division of Chemical Biology and Medicinal Chemistry, University of North Carolina School of Medicine, Chapel Hill, NC 27599, USA

⁷ These authors contributed equally: Yongfeng Liu, Can Cao

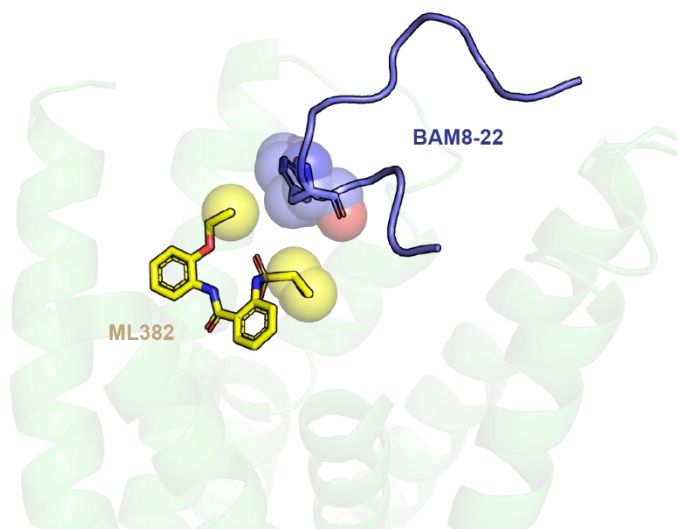
*Email: jfay@som.umaryland.edu; bryan_roth@med.unc.edu



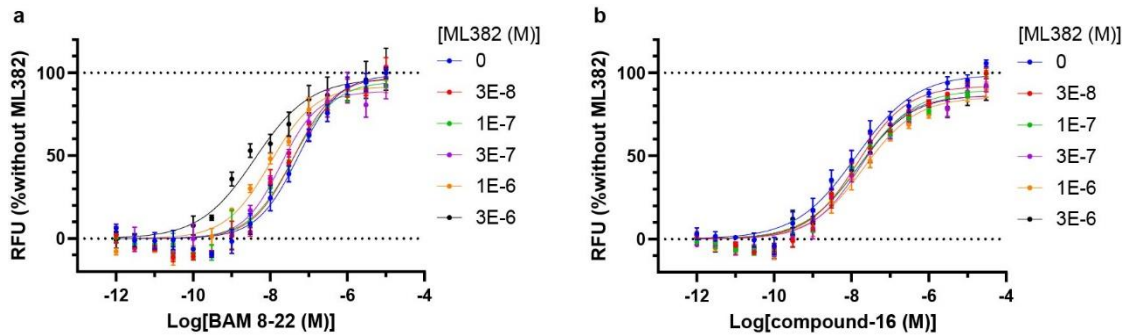
Supplementary Figure 1. Purification of the MRGPRX1-Gq complex. **a**, Representative size exclusion chromatography elution profile of the MRGPRX1-Gq complex. **b**, SDS-PAGE of samples of vitro reconstituted MRGPRX1-Gq complex. Full SDS-PAGE scans were shown at the end of supplementary information. Experiments were repeated three times with similar results.



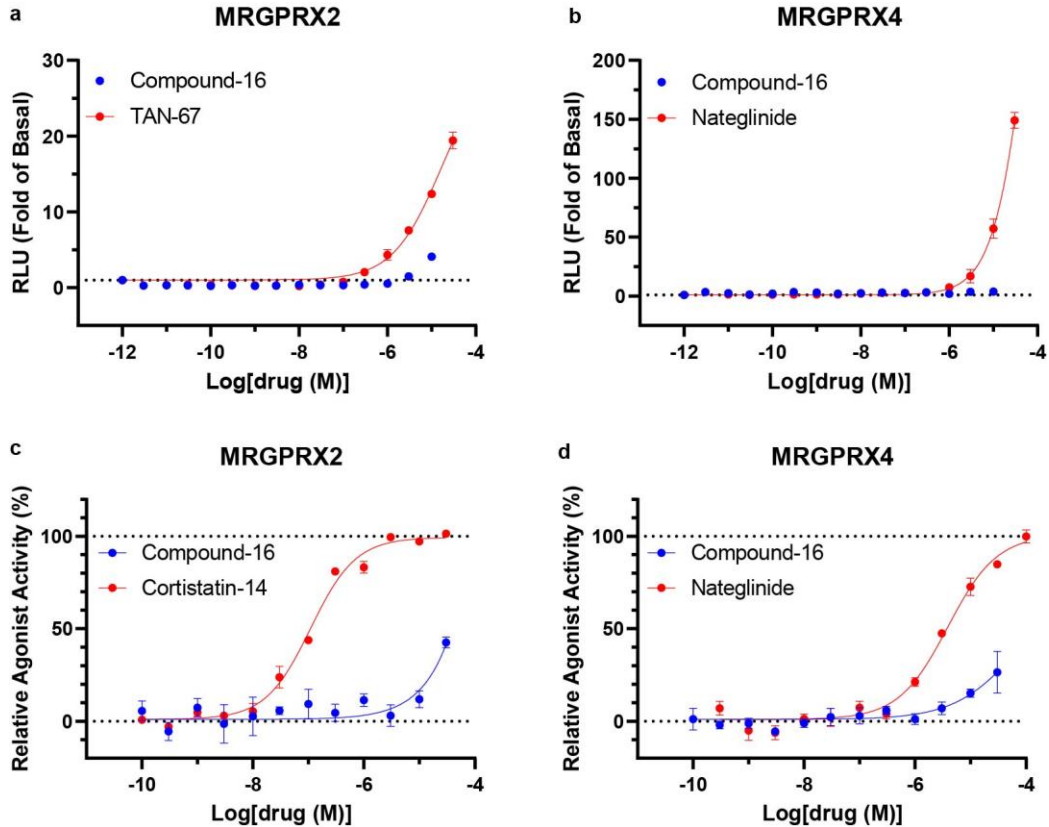
Supplementary Figure 2. Cryo-EM data processing flowcharts of MRGPRX1-Gq complex bound to BAM8-22, BAM8-22/ML382 and compound-16. The number of micrographs, particles and 3D classification of MRGPRX1-Gq complex bound to BAM8-22, BAM8-22/ML382 and compound-16 have been shown.



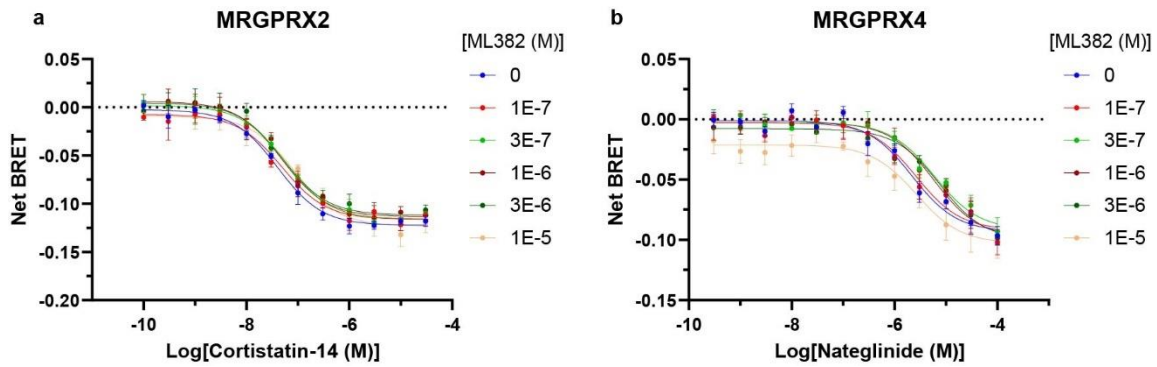
Supplementary Figure 3. The interactions between ML382 and the Tyr17 of BAM8-22. The upper part of 2-ethoxyphenyl and cyclopropyl sulfonamide groups of ML382 and Tyr17 of BAM8-22 are shown as spheres to highlight the hydrophobic interactions.



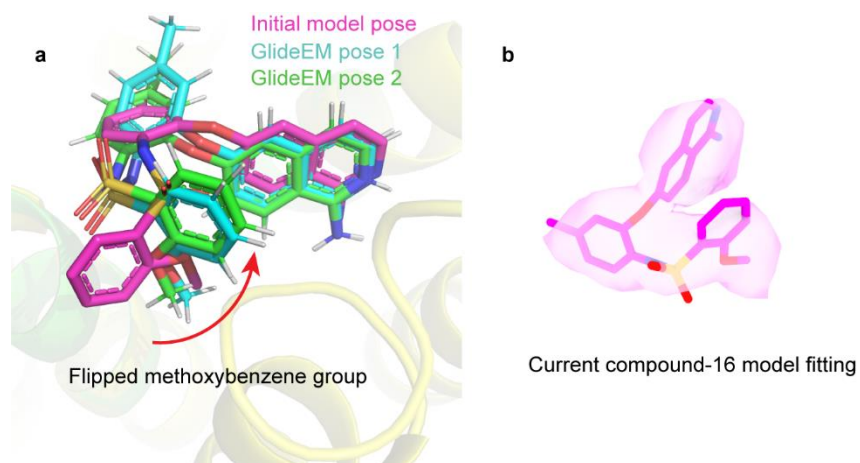
Supplementary Figure 4. Dose-response curves of MRGPRX1 with graded concentrations of ML382 using BAM8-22 and compound-16 as orthosteric ligands. Calcium mobilization assay was performed to assess ML382 allosteric regulation of BAM8-22 (a) and compound-16 (b), respectively. The data were presented as mean \pm SEM of $n=3$ biological replicates.



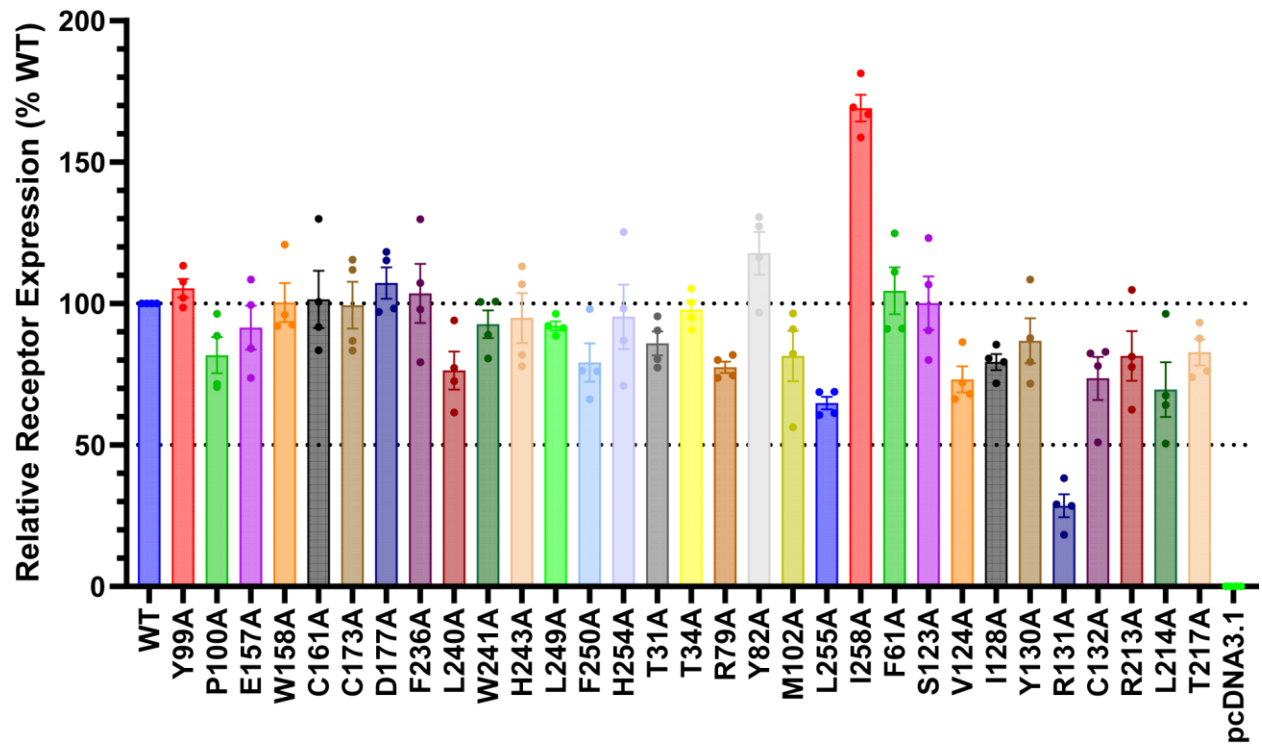
Supplementary Figure 5. Weak agonist activity of compound-16 with MRGPRX2 and MRGPRX4 receptors. Representative dose response curves for the MRGPRX2 and MRGPRX4 receptors in Tango assay (**a-b**) and BRET2 assay (**c-d**). Known agonists for MRGPRX2 (TAN-67 and cortistatin-14) and MRGPRX4 (nateglinide) were used as positive controls. The data were presented as mean \pm SEM of n=3 biological replicates.



Supplementary Figure 6. Allosteric activity of ML382 with other MRGPRX subtypes. In presence of Graded concentrations of ML382, Gq dissociate BRET2 assay was performed to assess ML382 allosteric regulation of cortistatin-14 with MRGPRX2 (**a**) or nateglinide with MRGPRX4 (**b**), respectively. The data were presented as mean \pm SEM of n=3 biological replicates.



Supplementary Figure 7. Validation of compound-16 pose. **a**, GlideEM docking result suggested compound-16 poses with the methoxybenzene group flipped are much more preferred in the current cryoEM map and MRGPRX1 model. **b**, The updated compound-16 pose could fit the ligand density well.



Supplementary Figure 8. Measurement of the cell surface expression level of WT and mutants of MRGPRX1 by ELISA. Data represent mean \pm SEM of n = 4 biological replicates.

Supplementary Table 1. Gαq dissociation (BRET2) parameter estimates for MRGPRX1 pocket mutations. EC₅₀ and E_{max} represents the average and standard error of the mean (SEM) from three independent experiments performed in duplicate. E_{max} is defined as percent WT maximum response. N.D., no detected activity as equilibrium could not be achieved at maximum agonist concentration for a reliable curve fitting.

MRGPRX1 Constructs	BAM8-22			Compound-16		
	pEC ₅₀ ± SEM	EC ₅₀ (μM)	E _{max} ± SEM, % WT	pEC ₅₀ ± SEM	EC ₅₀ (μM)	E _{max} ± SEM, % WT
WT	6.30 ± 0.04	0.50	100 ± 2	6.67 ± 0.07	0.21	100 ± 3
Y99A	5.14 ± 0.12	7.33	82 ± 9	N.D.	N.D.	<50
P100A	5.62 ± 0.07	2.38	119 ± 5	6.26 ± 0.06	0.54	100 ± 3
E157A	N.D.	N.D.	<50	N.D.	N.D.	<50
W158A	5.83 ± 0.05	1.49	101 ± 3	6.63 ± 0.07	0.23	101 ± 3
C161A	N.D.	N.D.	<50	N.D.	N.D.	<50
C173A	N.D.	N.D.	<50	N.D.	N.D.	<50
D177A	N.D.	N.D.	<50	N.D.	N.D.	<50
F236A	N.D.	N.D.	<50	N.D.	N.D.	N.D.
L240A	N.D.	N.D.	<50	6.11 ± 0.08	0.77	75 ± 3
W241A	N.D.	N.D.	<50	4.95 ± 0.24	11.1	66 ± 15
H243A	5.68 ± 0.07	0.61	98 ± 4	6.33 ± 0.07	0.46	96 ± 3
L249A	N.D.	N.D.	<50	5.10 ± 0.14	7.91	80 ± 9
F250A	N.D.	N.D.	<50	5.52 ± 0.12	2.99	70 ± 5
H254A	N.D.	N.D.	<50	5.92 ± 0.15	1.22	71 ± 6

Supplementary Table 2. Allosteric effect on WT and mutant MRGPRX1 using BRET2 dissociation assay. BRET dissociation assays were performed in the presence of increasing concentrations of BAM8-22 and ML382. Allosteric parameter (pK_B) obtained by fitting dose response curves to “Allosteric EC_{50} shift” function of Graphpad Prism 9.0. Data are presented as mean \pm SEM with $n = 3$ biological replicates. Greek letter delta (Δ) for the difference (ΔpEC_{50}) or affinity (ΔpK_B) when compared with the wild-type (WT) receptor values.

MRGPRX1 Constructs	BAM8-22		BAM8-22/10 μ M ML382		Allosteric	
	$pEC_{50} \pm$ SEM	ΔpEC_{50}	$pEC_{50} \pm$ SEM	ΔpEC_{50}	pK_B	ΔpK_B
WT	6.33 \pm 0.05	0	8.28 \pm 0.07	0	4.86 \pm 0.09	0
T31A	6.00 \pm 0.09	-0.36	7.20 \pm 0.06	-1.08	4.41 \pm 0.09	-0.45
T34A	5.63 \pm 0.11	-0.73	7.06 \pm 0.09	-1.22	4.46 \pm 0.13	-0.40
Y82A	6.11 \pm 0.07	-0.25	6.63 \pm 0.11	-1.65	3.62 \pm 0.10	-1.24
Y99A	5.40 \pm 0.10	-0.96	6.23 \pm 0.09	-2.05	3.81 \pm 0.11	-1.05
M102A	5.70 \pm 0.09	-0.66	7.24 \pm 0.08	-1.04	4.55 \pm 0.11	-0.31
H254A	N.D.	N.D.	6.53 \pm 0.09	-1.75	4.34 \pm 0.06	-0.52
I258A	5.85 \pm 0.07	-0.51	6.21 \pm 0.08	-2.07	3.24 \pm 0.09	-1.62

Supplementary Table 3. The MRGPRX1 and Gq protein interface mutations tested in BRET2 dissociation assay. EC_{50} and E_{max} estimates represent the average and standard error of the mean (SEM) from three independent experiments performed in triplicate. E_{max} is defined as percent WT maximum response. N.D.; no detected activity as equilibrium could not be achieved at maximum agonist concentration for a reliable curve fitting.

MRGPRX1 Constructs	Compound-16			BAM8-22			BAM8-22 + 1 μ M ML382		
	$pEC_{50} \pm$ SEM	EC_{50} (μ M)	$E_{max} \pm$ SEM, % WT	$pEC_{50} \pm$ SEM	EC_{50} (μ M)	$E_{max} \pm$ SEM, % WT	$pEC_{50} \pm$ SEM	EC_{50} (μ M)	$E_{max} \pm$ SEM, % WT
WT	6.68 \pm 0.05	0.21	100 \pm 2	6.23 \pm 0.04	0.59	100 \pm 2	7.15 \pm 0.03	0.07	100 \pm 1
F61A	6.09 \pm 0.06	0.81	94 \pm 3	5.57 \pm 0.08	2.70	91 \pm 5	6.78 \pm 0.05	0.17	99 \pm 2
S123A	6.83 \pm 0.05	0.15	104 \pm 2	6.07 \pm 0.05	0.85	101 \pm 3	6.96 \pm 0.04	0.11	99 \pm 2
V124A	5.84 \pm 0.07	1.46	76 \pm 3	5.42 \pm 0.10	3.83	77 \pm 6	6.64 \pm 0.05	0.23	88 \pm 2
I128A	4.66 \pm 0.25	22.1	58 \pm 17	N.D.	N.D.	<50	N.D.	N.D.	<50
Y130A	6.50 \pm 0.05	0.31	98 \pm 2	5.96 \pm 0.07	1.09	93 \pm 5	7.00 \pm 0.05	0.10	86 \pm 2
R131A	N.D.	N.D.	<50	N.D.	N.D.	<50	N.D.	N.D.	<50
C132A	5.25 \pm 0.14	5.60	63 \pm 7	5.23 \pm 0.13	5.92	60 \pm 7	6.47 \pm 0.08	0.34	63 \pm 3
R213A	7.38 \pm 0.03	0.04	105 \pm 2	6.66 \pm 0.04	0.22	116 \pm 2	7.32 \pm 0.03	0.05	106 \pm 2
L214A	5.84 \pm 0.07	1.44	68 \pm 3	5.56 \pm 0.10	2.78	67 \pm 6	6.68 \pm 0.05	0.21	89 \pm 2
T217A	7.11 \pm 0.04	0.08	105 \pm 2	6.45 \pm 0.04	0.36	123 \pm 2	7.23 \pm 0.04	0.06	106 \pm 2

Supplementary Table 4. The sequences of primers that used for generating the MRGPRX1 mutations.

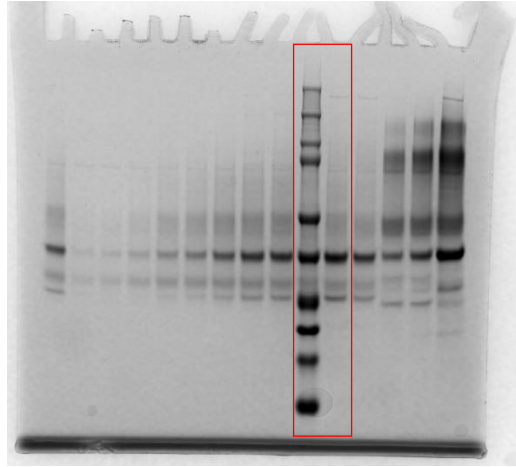
Name	5'-Sequence-3'
MRGPRX1_T31A_Fwd	GTCCTTg _g CTGTCCTCACCTGTATTGTAAGTCTGGTG
MRGPRX1_T31A_Rev	GAGGACAGcCAAGGACAGTGTGGCTTGTAAACAAAG
MRGPRX1_T34A_Fwd	GTCCTCg _g CCTGTATTGTAAGTCTGGTGGGGCTGAC
MRGPRX1_T34A_Rev	CAATACAGGcGAGGACAGTCAAGGACAGTGTGGCTTG
MRGPRX1_F61A_Fwd	GAATGCTg _c CTCCATTTACATACTGAACCTCGCCG
MRGPRX1_F61A_Rev	AATGGAGg _c AGCATTCCGTCGCATCCGGCAACCCAG
MRGPRX1_R79A_Fwd	CTCAGGGg _c ACTTATCTACAGCCTTTTGTCTTTTATC
MRGPRX1_R79A_Rev	GATAAGTg _c CCCTGAGAGGAAAAGGAAATCAGCAG
MRGPRX1_Y82A_Fwd	CTTATCg _c CAGCCTTTTGTCTTTTATCAGCATT
MRGPRX1_Y82A_Rev	AAGGCTGg _c GATAAGTCTCCCTGAGAGGAAAAG
MRGPRX1_Y99A_Fwd	GATCCTGg _c CCGGTCATGATGTTTTCTTACTTC
MRGPRX1_Y99A_Rev	GACCGGGg _c CAGGATCTTGGAAATTGTATGTGGAATG
MRGPRX1_P100A_Fwd	CTGTACg _g CGGTCATGATGTTTTCTTACTTCGCC
MRGPRX1_P100A_Rev	CATGACCGcGTACAGGATCTTGGAAATTGTATG
MRGPRX1_M102A_Fwd	CCGGTCg _c GATGTTTTCTTACTTCGCCGGCCTGTC
MRGPRX1_M102A_Rev	GAAAACATCg _c GACCGGGTACAGGATCTTGGAAATTG
MRGPRX1_S123A_Fwd	TGTCTGg _c TGTCCTCTGGCCGATTTGGTATAGGTG
MRGPRX1_S123A_Rev	GAGGACAg _c CAGACATCTTCCGTGGAGACTGCAC
MRGPRX1_V124A_Fwd	CTGTCTGcCCTCTGGCCGATTTGGTATAGGTGTC
MRGPRX1_V124A_Rev	CCAGAGGg _c CAGACAGACATCTTCCGTGGAGAC
MRGPRX1_I128A_Fwd	TGGCCGg _c TTGGTATAGGTGTTCATAGGCCGACTC
MRGPRX1_I128A_Rev	ATACCAAg _c CGGCCAGAGGACAGACAGACATCTTTC
MRGPRX1_Y130A_Fwd	GATTTGGg _c TAGGTGTATAGGCCGACTCACCTG
MRGPRX1_Y130A_Rev	GACACCTAg _c CAAATCGGCCAGAGGACAGACAG
MRGPRX1_R131A_Fwd	TGGTATg _c GTGTATAGGCCGACTCACCTGAGTG
MRGPRX1_R131A_Rev	ATGACACg _c ATACCAAATCGGCCAGAGGACAGAC
MRGPRX1_C132A_Fwd	GTATAGGg _c TCATAGGCCGACTCACCTGAGTGCCG
MRGPRX1_C132A_Rev	CCTATGAg _c CCTATACCAAATCGGCCAGAGGACAG
MRGPRX1_E157A_Fwd	ATACTGGcGTGGATGCTGTGTGGATTTCTCTTTAGTG
MRGPRX1_E157A_Rev	CATCCACg _c CCAGTATAGACCCGAGAAGGGAGAGG
MRGPRX1_W158A_Fwd	CTGGAGg _c GATGCTGTGTGGATTTCTCTTTAGTG
MRGPRX1_W158A_Rev	CAGCATCg _c CTCCAGTATAGACCCGAGAAGGGAG
MRGPRX1_C161A_Fwd	ATGCTGg _c TGGATTTCTCTTTAGTGGTCCGACTC
MRGPRX1_C161A_Rev	GAAATCCAg _c CAGCATCCACTCCAGTATAGACC
MRGPRX1_C173A_Fwd	GCATGGg _c TCAGACCAGTGATTTTATCACTGTC
MRGPRX1_C173A_Rev	GGTCTGAg _c CCATGCAGAGTCGGCACCCTAAAGAG
MRGPRX1_D177A_Fwd	ACCAGTGcTTTTATCACTGTCGCTGGCTTATTTTC
MRGPRX1_D177A_Rev	GATAAAAg _c CACTGGTCTGACACCATGCAGAGTCGGCAC
MRGPRX1_R213A_Fwd	CTGACAg _c CCTGTACGTGACCATCCTTCTGACGG
MRGPRX1_R213A_Rev	GTACAGGg _c TGTCAGTGGGATTTTGGGGCTGCCAC
MRGPRX1_L214A_Fwd	GACACGCg _c GTACGTGACCATCCTTCTGACGGTA
MRGPRX1_L214A_Rev	CACGTACg _c GCGTGTGAGTGGGATTTTGGGGCTG
MRGPRX1_T217A_Fwd	GTACGTGg _c CCATCCTTCTGACGGTATTGGTGTT
MRGPRX1_T217A_Rev	GAAGGATGGcCACGTACAGGCGTGTGAGTGGGATTTTG
MRGPRX1_F232A_Fwd	TTGCCTg _c CGGGATCCAATTCTTCTTCTTCTCTG
MRGPRX1_F232A_Rev	GATCCCGg _c AGGCAAACACACAGGAGGAACACC
MRGPRX1_F236A_Fwd	GATCCAAg _c CTTCTTCTTCTGATACACGTC
MRGPRX1_F236A_Rev	GAGGAAGg _c TTGGATCCCGAAAAGCAAACACAC
MRGPRX1_L240A_Fwd	CTTCTGc _c CTGGATACACGTGGATCGGGAAGTG
MRGPRX1_L240A_Rev	GTATCCAGg _c GAAGAGGAAGAATTGGATCCCGAAAAG
MRGPRX1_W241A_Fwd	CTTCTCg _c GATACACGTGGATCGGGAAGTGCTTTTC
MRGPRX1_W241A_Rev	GTGTATCg _c GAGGAAGAGGAAGAATTGGATCCCGAAAAG
MRGPRX1_L249A_Fwd	GAAGTGg _c TTTTCTGCCACGTTACCTGGTGAGTATC
MRGPRX1_L249A_Rev	GCAGAAAg _c CACTTCCCGATCCACGTGTATCCAG

MRGPRX1_F250A_Fwd	GTGCTTgcCTGCCACGTTACCTGGTGAGTATCTTTC
MRGPRX1_F250A_Rev	GTGGCAGgcAAGCACTTCCCGATCCACGTGTATCCAG
MRGPRX1_H254A_Fwd	CACGTTgcCCTGGTGAGTATCTTTCTGTCCGCACTG
MRGPRX1_H254A_Rev	CACCAGGgcAACGTGGCAGAAAAGCACTTCCCGATC
MRGPRX1_L255A_Fwd	GTTCACgcGGTGAGTATCTTTCTGTCCGCACTG
MRGPRX1_L255A_Rev	ACTCACgcGTGAACGTGGCAGAAAAGCACTTC
MRGPRX1_I258A_Fwd	GTGAGTgcCTTTCTGTCCGCACTGAATAGCAGCGC
MRGPRX1_I258A_Rev	CAGAAAGgcACTCACCAGGTGAACGTGGCAGAAAAG

Supplementary Table 5. Cryo-EM data collection, refinement, and validation statistics.

	MRGPRX1-Gq BAM8-22 (EMD-27752) (PDB 8DWC)	MRGPRX1-Gq BAM8-22/ML382 (EMD-27753) (PDB 8DWG)	MRGPRX1-Gq Compound-16 (EMD- 27754) (PDB 8DWH)
Data collection and processing			
Magnification	45,000	45,000	45,000
Voltage (kV)	200	200	200
Electron exposure (e ⁻ /Å ²)	44.5	44.5	43.8
Number of movies used	3801	2495	3218
Defocus mean (SD) μm ¹	1.4 (0.5)	1.3 (0.3)	1.5 (0.5)
Range	0.1-3.3	0.2-2.4	0.1-3.6
Pixel size (Å)	0.88	0.88	0.88
Symmetry imposed	C1	C1	C1
Initial particle images (no.)	2,246,376	402,342	176,422
Final particle images (no.)	652,843	290,962	116,978
Map resolution (Å) ²	2.87	2.71	3.25
FSC threshold	0.143	0.143	0.143
Map resolution range (Å)	2.5-4.7	2.3-5.1	2.8-6.6
Refinement			
Initial model used (PDB code)	7S8N	7S8N	7S8N
Model resolution (Å)	3.01	2.88	3.58
FSC threshold	0.5	0.5	0.5
Map sharpening B factor (Å ²)	110.5	76.6	89.4
Model composition			
Non-hydrogen atoms	8298	8350	6444
Protein residues	1102	1101	858
Ligands	/	1	1
<i>B</i> factors (Å ²)			
Protein	52.92	50.63	60.77
Ligand	/	49.92	61.66
R.m.s. deviations			
Bond lengths (Å)	0.008	0.005	0.004
Bond angles (°)	0.637	0.590	0.551
Validation			
MolProbity score	1.73	1.68	1.64
Clashscore	7.22	6.56	7.56
Poor rotamers (%)	0.00	0.00	0.00
Ramachandran plot			
Favored (%)	0.00	0.00	0.00
Allowed (%)	4.81	4.53	3.44
Disallowed (%)	95.19	95.47	96.56

1 underfocus positive 2 Resolution estimates from cryoSPARC auto-corrected GSFSC



The unprocessed scan of the SDS-PAGE gel. The Supplementary Figure 1b is shown in the red frame.